Iridoid Synthase Activity Is Common among the Plant Progesterone 5β-Reductase Family

Jennifer Munkert[1], Jacob Pollier[2,3], Karel Miettinen[4], Alex Van Moerkercke[2,3], Richard Payne[5], Frieder Müller-Uri[1], Vincent Burlat[6,7], Sarah E. O'Connor[5], Johan Memelink[4], Wolfgang Kreis[1,*] and Alain Goossens[2,3,*]

[1]Department of Biology, University of Erlangen-Nuremberg, 91058 Erlangen, Germany

[2]Department of Plant Systems Biology, VIB, 9052 Gent, Belgium

[3]Department of Plant Biotechnology and Bioinformatics, Ghent University, 9052 Gent, Belgium

[4]Sylvius Laboratory, Institute of Biology Leiden, Leiden University, Leiden 2333 BE, The Netherlands

[5]Department of Biological Chemistry, John Innes Centre, Norwich NR4 7UH, UK

[6]Université de Toulouse, UPS, UMR 5546, Laboratoire de Recherche en Sciences Végétales, BP 42617 Auzeville, F-31326 Castanet-Tolosan, France

[7]CNRS, UMR 5546, BP 42617, F-31326 Castanet-Tolosan, France

*Correspondence: Wolfgang Kreis (wolfgang.kreis@fau.de), Alain Goossens (alain.goossens@psb.vib-ugent.be)

http://dx.doi.org/10.1016/j.molp.2014.11.005

ABSTRACT

***Catharanthus roseus*, the Madagascar periwinkle, synthesizes bioactive monoterpenoid indole alkaloids, including the anti-cancer drugs vinblastine and vincristine. The monoterpenoid branch of the alkaloid pathway leads to the secoiridoid secologanin and involves the enzyme iridoid synthase (IS), a member of the progesterone 5β-reductase (P5βR) family. IS reduces 8-oxogeranial to iridodial. Through transcriptome mining, we show that *IS* belongs to a family of six *C. roseus P5βR* genes. Characterization of recombinant CrP5βR proteins demonstrates that all but CrP5βR3 can reduce progesterone and thus can be classified as P5βRs. Three of them, namely CrP5βR1, CrP5βR2, and CrP5βR4, can also reduce 8-oxogeranial, pointing to a possible redundancy with IS (corresponding to CrP5βR5) in secoiridoid synthesis. In-depth functional analysis by subcellular protein localization, gene expression analysis, *in situ* hybridization, and virus-induced gene silencing indicate that besides IS, CrP5βR4 may also participate in secoiridoid biosynthesis. We cloned a set of *P5βR* genes from angiosperm plant species not known to produce iridoids and demonstrate that the corresponding recombinant proteins are also capable of using 8-oxogeranial as a substrate. This suggests that IS activity is intrinsic to angiosperm P5βR proteins and has evolved early during evolution.**

Key words: *Catharanthus roseus*, *Medicago truncatula*, progesterone reductase, secoiridoid, monoterpenoid indole alkaloid, *VEP1*-encoded enone-reductases

INTRODUCTION

Plants produce a wide range of specialized metabolites including the large classes of terpenoids and alkaloids, the source of many bioactive compounds that help plants to survive in their environment with interesting human applications. The evolution of the corresponding biosynthetic pathways required the evolution of new genes, for instance encoding enzymes with new activities or substrate specificities, which mainly occurred through gene duplications with successive diversifications and neofunctionalizations (Ober, 2010). The advent of ever cheaper and faster next-generation sequencing technologies in the past decade has led to the generation of massive gene lists gathered from genomes and transcriptomes of numerous model, crop, medicinal, and other plant species. These offer unprecedented catalogs of enzyme-encoding genes, which can be used in synthetic biology programs and in the study of pathway evolution. This is well illustrated by the cytochrome P450 (P450) family, which appears to form the largest superfamily of enzymes, essentially due to its expansion in plants. P450s catalyze most of the rate-limiting

and irreversible reactions in plant-specific specialized metabolic pathways but are also involved in primary metabolic house-keeping functions, such as the synthesis of sterols, fatty acids, hormones, and other signaling molecules (Schuler and Werck-Reichhart, 2003; Renault et al., 2014).

Another protein superfamily linked to plant-specialized metabolism is that of the short-chain dehydrogenases/reductases (SDR), which include the Vein Patterning 1 (VEP1)-encoded enone-reductases (Jörnvall et al., 1995; Kavanagh et al., 2008). The latter enzymes were first isolated from cardenolide-producing plants and termed progesterone 5β-reductases (P5βRs) because they enantioselectively convert progesterone, a precursor in cardenolide biosynthesis, to 5β-pregnane-3,20-dione (Gärtner et al., 1994). Meanwhile, *P5βR* genes have not only been identified in cardenolide-producing plant species, such as *Digitalis lanata* and *Erysimum crepidifolium*, but also in cardenolide-free plants, such as *Arabidopsis thaliana.* Today, over 100 distinct plant *P5βR* genes can be found in the NCBI database, generally with several paralogs from a single species (see e.g., http://www.ncbi.nlm.nih.gov/nuccore/). *P5βR* likely originated in an α-proteobacterium and is thought to have been laterally propagated through nets of ecological interactions (Tarrío et al., 2011). Several *P5βR* cDNAs have been functionally expressed in *Escherichia coli* and the corresponding recombinant enzymes are capable of reducing a large variety of substrates bearing an active C = C double bond by a 1,4-addition mechanism using NADPH as the co-substrate (Herl et al., 2006; Gavidia et al., 2007; Burda et al., 2009; Herl et al., 2009; Bauer et al., 2010; Munkert et al., 2011; Durchschein et al., 2012).

The wide occurrence of functional P5βRs within the angiosperm lineage (Bauer et al., 2010) and their relaxed substrate specificity raised the question whether P5βRs are involved in more biosynthetic pathways than previously assumed. Indeed, a P5βR homolog, denominated iridoid synthase (IS), was recently isolated from *Catharanthus roseus* (JX974564) and reported to be involved in secoiridoid biosynthesis, since it was able to reduce 8-oxogeranial and form iridodial (Geu-Flores et al., 2012; Supplemental Figure 1). It was suggested that after the 1,4-addition reduction of 8-oxogeranial, an enol intermediate would be formed that is further converted into iridodial, either through a cycloaddition via an inverse-electron demand Diels–Alder reaction or through an intramolecular Michael addition.

The secoiridoid pathway is a monoterpenoid pathway that was recently fully elucidated (Geu-Flores et al., 2012; Asada et al., 2013; Salim et al., 2013; Miettinen et al., 2014; Salim et al., 2014). It starts with geraniol, comprises eight enzymes, including IS, that catalyze successive oxidation, reduction, glycosylation, and methylation reactions, and leads to secologanin as the branch end point. Secologanin is coupled to tryptamine by strictosidine synthase to form strictosidine, the universal precursor of the monoterpenoid indole alkaloids (MIAs), which are synthesized in a wide variety of plants. Many (seco)iridoids and MIAs have valuable bioactivities, including the well-known molecules vinblastine and vincristine from *C. roseus*, which are used for the treatment of several types of cancer.

In this study, we mined public *C. roseus* transcriptome databases and identified five other genes that show high sequence similarity to *IS* and the other *P5βR* entries in the NCBI database. All of them were cloned and functionally characterized. We assessed their substrate specificities to determine whether all are able to reduce progesterone, small enones, as well as the IS substrate 8-oxogeranial. Furthermore, we analyzed their subcellular accumulation, expression patterns, and *in planta* activity to investigate their participation in MIA biosynthesis in *C. roseus* plants. Finally, we cloned *P5βRs* from other, non–iridoid-producing angiosperm species and assessed their capacity to reduce 8-oxogeranial.

RESULTS

Identification of Six *P5βR* Genes in *C. roseus*

Previously, we have reported on CathaCyc, a metabolic pathway database from *C. roseus* built from RNA-Seq data (www.cathacyc.org; Van Moerkercke et al., 2013). We screened this transcriptome database for candidate *P5βRs* by performing a TBLASTN search with a previously characterized *P5βR* from *D. lanata* (GenBank accession number, AAS76634; Herl et al., 2006). Contigs corresponding to five full-length and several partial *P5βRs* were identified. To obtain the full-length open reading frames of the partial *P5βR* sequences, a BLASTN search with the partial sequences was performed in the *C. roseus* transcriptome database from the Medicinal Plant Genomics Resource (MPGR) consortium (http://medicinalplantgenomics.msu.edu/), leading to the identification of a sixth full-length *P5βR* sequence. The *P5βR* sequences identified were denominated *CrP5βR1* to *CrP5βR6* (Figure 1), with *CrP5βR1* and *CrP5βR6* showing highest and lowest sequence similarity to *DIP5βR*, respectively, and with *CrP5βR5* corresponding to the recently characterized *IS* (GenBank accession number, JX974564) involved in MIA biosynthesis (Geu-Flores et al., 2012). To avoid confusion, we suggest using the acronym P5βR and adding a two-letter code indicating the plant origin and a consecutive number if more than one gene is present in a given species.
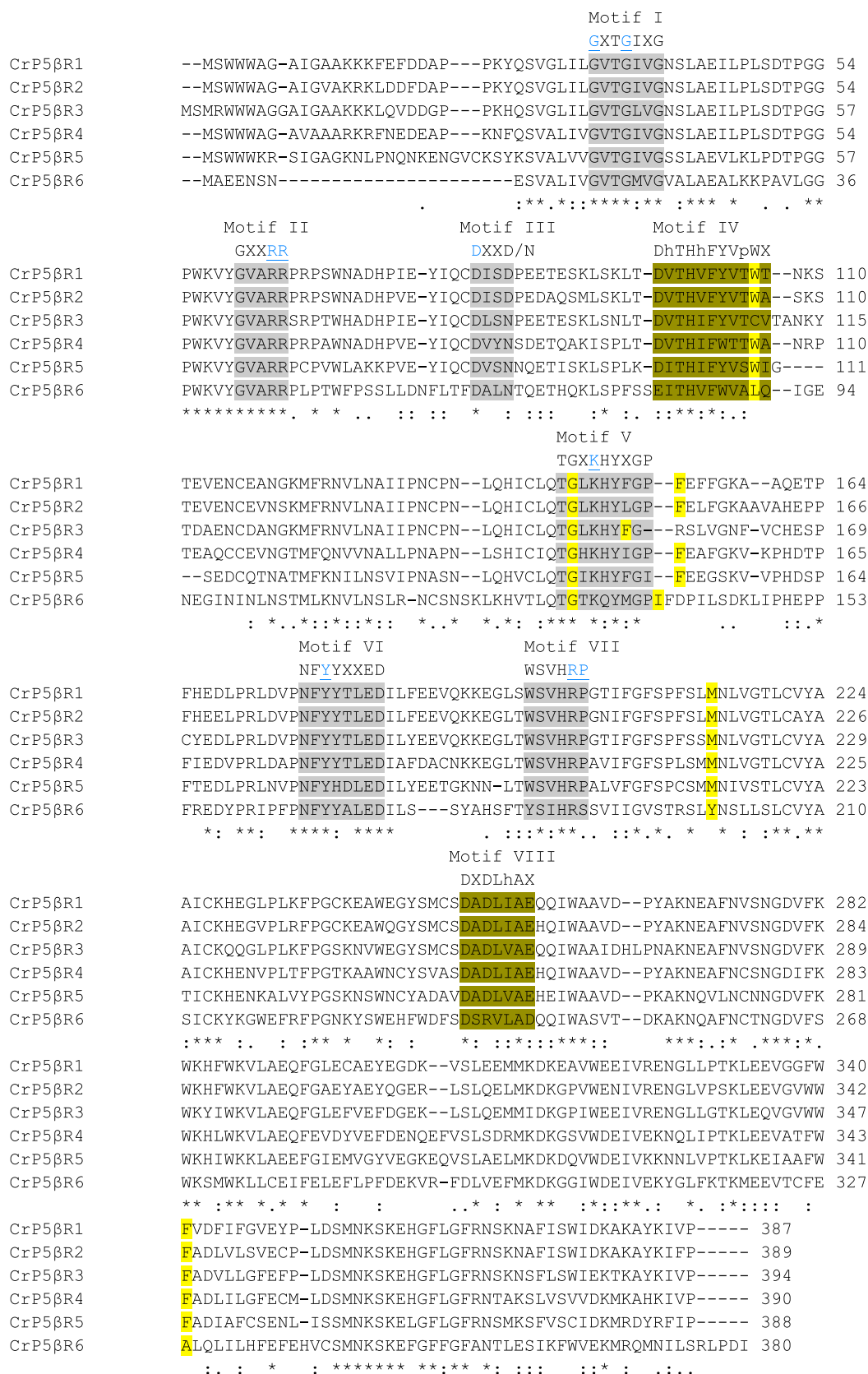
Phylogenetic Analysis of the CrP5βRs

The six *C. roseus* P5βRs isolated showed a sequence identity between 41% and 87% at the amino acid level, which was similar to the range when compared to P5βRs from other species, such as At4g24220, At5g58750, DIP5βR1 (AAS93804), DIP5βR2 (ADL28122), EcP5βR1 (ADG56544), and EcP5βR2, which had a sequence identity between 41% and 78%.

A phylogenetic analysis using the full-length amino acid sequences from the P5βRs from *C. roseus* and other plants demonstrated that the P5βR family can be clustered into at least two groups, which we termed P5βR cluster I and cluster II (Figure 2). Cluster I contains the *C. roseus* CrP5βR1, CrP5βR2, CrP5βR3, and CrP5βR4, which cluster together with DIP5βR1 (AAS76634), EcP5βR1 (ADG56544), and *Arabidopsis* At4g24220 (VEP1). CrP5βR5/IS and CrP5βR6, on the other hand, cluster together with DIP5βR2 (ADL28122) and *Arabidopsis* At5g58750. Thus, *P5βR* genes residing in one genome have paralogous sequences.

Characterization of Recombinant CrP5βR Proteins Produced in *E. coli*

Paralogs may have similar functions or activities. To test this assumption, cDNA corresponding to all *CrP5βR* genes was

```
                                                                Motif I
                                                                GXTGIXG
CrP5βR1     --MSWWWAG-AIGAAKKKFEFDDAP---PKYQSVGLILGVTGIVGNSLAEILPLSDTPGG 54
CrP5βR2     --MSWWWAG-AIGVAKRKLDDFDAP---PKYQSVGLILGVTGIVGNSLAEILPLSDTPGG 54
CrP5βR3     MSMRWWWAGGAIGAAKKKLQVDDGP--PKHQSVGLILGVTGLVGNSLAEILPLSDTPGG 57
CrP5βR4     --MSWWWAG-AVAAARKRFNEDEAP---KNFQSVALIVGVTGIVGNSLAEILPLSDTPGG 54
CrP5βR5     --MSWWWKR-SIGAGKNLPNQNKENGVCKSYKSVALVVGVTGIVGSSLAEVLKLPDTPGG 57
CrP5βR6     --MAEENSN--------------------ESVALIVGVTGMVGVALAEALKKPAVLGG 36
                            .        :**.*::*****:** :*** *   .  . **

            Motif II                      Motif III           Motif IV
            GXXRR                         DXXD/N               DhTHhFYVpWX
CrP5βR1     PWKVYGVARRPRPSWNADHPIE-YIQCDISDPEETESKLSKLT-DVTHVFYVTWT--NKS 110
CrP5βR2     PWKVYGVARRPRPSWNADHPVE-YIQCDISDPEDAQSMLSKLT-DVTHVFYVTWA--SKS 110
CrP5βR3     PWKVYGVARRSRPTWHADHPIE-YIQCDLSNPEETESKLSNLT-DVTHIFYVTCVTANKY 115
CrP5βR4     PWKVYGVARRPRPAWNADHPVE-YIQCDVYNSDETQAKISPLT-DVTHIFWTTWA--NRP 110
CrP5βR5     PWKVYGVARRPCPVWLAKKPVE-YIQCDVSNNQETISKLSPLK-DITHIFYVSWIG---- 111
CrP5βR6     PWKVYGVARRPLPTWFPSSLLDNFLTFDALNTQETHQKLSPFSSEITHVFWVALQ--IGE 94
            **********. * *  ..  :: ::   *  : :::   :*  :. ::**:*:.:

                                            Motif V
                                            TGXKHYXGP
CrP5βR1     TEVENCEANGKMFRNVLNAIIPNCPN--LQHICLQTGLKHYFGP--FEFFGKA--AQETP 164
CrP5βR2     TEVENCEVNSKMFRNVLNAIIPNCPN--LQHICLQTGLKHYLGP--FELFGKAAVAHEPP 166
CrP5βR3     TDAENCDANGKMFRNVLNAIIPNCPN--LQHICLQTGLKHYFG---RSLVGNF-VCHESP 169
CrP5βR4     TEAQCCEVNGTMFQNVVNALLPNAPN--LSHICIQTGHKHYIGP--FEAFGKV-KPHDTP 165
CrP5βR5     --SEDCQTNATMFKNILNSVIPNASN--LQHVCLQTGIKHYFI--FEEGSKV-VPHDSP 164
CrP5βR6     NEGININLNSTMLKNVLNSLR-NCSNSKLKHVTLQTGTKQYMGPIFDPILSDKLIPHEPP 153
              : *..*::*::*::  *..*  *.*: :*** *:*:*      ..    ::.*

            Motif VI          Motif VII
            NFYYXXED          WSVHRP
CrP5βR1     FHEDLPRLDVPNFYYTLEDILFEEVQKKEGLSWSVHRPGTIFGFSPFSLMNLVGTLCVYA 224
CrP5βR2     FHEELPRLDVPNFYYTLEDILFEEVQKKEGLTWSVHRPGNIFGFSPFSLMNLVGTLCAYA 226
CrP5βR3     CYEDLPRLDVPNFYYTLEDILYEEVQKKEGLTWSVHRPGTIFGFSPFSSMNLVGTLCVYA 229
CrP5βR4     FIEDVPRLDAPNFYYTLEDIAFDACNKKEGLTWSVHRPAVIFGFSPLSMMNLVGTLCVYA 225
CrP5βR5     FTEDLPRLNVPNFYHDLEDILYEETGKNN-LTWSVHRPALVFGFSPCSMMNIVSTLCVYA 223
CrP5βR6     FREDYPRIPFPNFYYALEDILS---SYAHSFTYSIHRSSVIIGVSTRSLYNSLLSLCVYA 210
              *: **:  ****: ****  . :::*:**.. ::*.*. *  * : :**.**

                            Motif VIII
                            DXDLhAX
CrP5βR1     AICKHEGLPLKFPGCKEAWEGYSMCSDADLIAEQQIWAAVD--PYAKNEAFNVSNGDVFK 282
CrP5βR2     AICKHEGVPLRFPGCKEAWQGYSMCSDADLIAEHQIWAAVD--PYAKNEAFNVSNGDVFK 284
CrP5βR3     AICKQQGLPLKFPGSKNVWEGYSMCSDADLVAEQQIWAAIDHLPNAKNEAFNVSNGDVFK 289
CrP5βR4     AICKHENVPLTFPGTKAAWNCYSVASDADLIAEHQIWAAVD--PYAKNEAFNCSNGDIFK 283
CrP5βR5     TICKHENKALVYPGSKNSWNCYADAVDADLVAEHEIWAAVD--PKAKNQVLNCNNGDVFK 281
CrP5βR6     SICKYKGWEFRFPGNKYSWEHFWDFSDSRVLADQQIWASVT--DKAKNQAFNCTNGDVFS 268
            :*** :.  : :** *  *: :   *: ::*:::***::    ***:.:* .***:*.

CrP5βR1     WKHFWKVLAEQFGLECAEYEGDK--VSLEEMMKDKEAVWEEIVRENGLLPTKLEEVGGFW 340
CrP5βR2     WKHFWKVLAEQFGAEYAEYQGER--LSLQELMKDKGPVWENIVRENGLVPSKLEEVGVWW 342
CrP5βR3     WKYIWKVLAEQFGLEFVEFDGEK--LSLQEMMIDKGPIWEEIVRENGLLGTKLEQVGVWW 347
CrP5βR4     WKHLWKVLAEQFEVDYVEFDENQEFVSLSDRMKDKGSVWDEIVEKNQLIPTKLEEVATFW 343
CrP5βR5     WKHIWKKLAEEFGIEMVGYVEGKEQVSLAELMKDKDQVWDEIVKKNNLVPTKLKEIAAFW 341
CrP5βR6     WKSMWKLLCEIFELEFLPFDEKVR-FDLVEFMKDKGGIWDEIVEKYGLFKTKMEEVTCFE 327
            ** :** *.* *  :    :    ..* : * **  :*::**.:  *. :*::::  :

CrP5βR1     FVDFIFGVEYP-LDSMNKSKEHGFLGFRNSKNAFISWIDKAKAYKIVP----- 387
CrP5βR2     FADLVLSVECP-LDSMNKSKEHGFLGFRNSKNAFISWIDKAKAYKIFP----- 389
CrP5βR3     FADVLLGFEFP-LDSMNKSKEHGFLGFRNSKNSFLSWIEKTKAYKIVP----- 394
CrP5βR4     FADLILGFECM-LDSMNKSKEHGFLGFRNTAKSLVSVVDKMKAHKIVP----- 390
CrP5βR5     FADIAFCSENL-ISSMNKSKELGFLGFRNSMKSFVSCIDKMRDYRFIP----- 388
CrP5βR6     ALQLILHFEFEHVCSMNKSKEFGFFGFANTLESIKFWVEKMRQMNILSRLPDI 380
            :. :  *   : ******* **:** *: :::   ::* :  .:...
```

Figure 1. Alignment of the Amino Acid Sequences of the Progesterone 5β-Reductases (P5βRs) of *C. roseus* (CrP5βR1–CrP5βR6).
Conserved amino acid motifs after Thorn et al. (2008) are shown in gray and two additional motifs identified by Pérez-Bermúdez et al. (2010) are shown in dark green, as well as catalytically important amino acids after Bauer et al. (2010) in yellow.
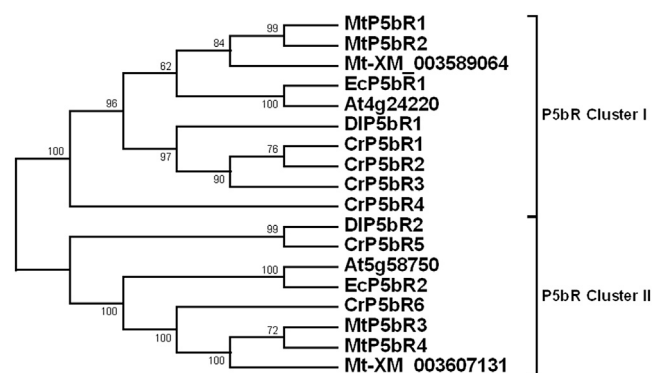
Figure 2. Cladogram of Different P5βR Amino Acid Sequences Generated by MEGA 4.
The evolutionary history was inferred using the Neighbor-Joining method. The optimal tree with the sum of branch length 3.45318782 is shown. The percentage of replicate trees, in which the associated taxa clustered together in the bootstrap test (1000 replicates), is shown next to the branches. The evolutionary distances were computed using the Poisson correction method and are in the units of the number of amino acid substitutions per site. All positions containing gaps and missing data were eliminated from the data set (Complete deletion option). There were a total of 353 positions in the final data set. Cluster I includes P5βR from *M. truncatula* (MtP5βR1, XM_003638410; MtP5βR1, XM_003638414) as well as CrP5βR1–4, EcP5βR1 (ADG56544), DIP5βR1 (AAS93804), and At4g24220. Cluster II contains CrP5βR5-6, At5g58750, EcP5βR2, DIP5βR2 (ADL28122), and two *M. truncatula* reductases (MtP5βR3, XM_003609687; MtP5βR4, XM_003609689).

isolated and expressed in *E. coli*. Recombinant enzymes could be produced in sufficient amounts to allow further characterization of CrP5βR1, CrP5βR2, CrP5βR4, CrP5βR5, and CrP5βR6, but not of CrP5βR3 (Figure 3).

The kinetic data for the substrates progesterone, 2-cyclohexen-1-one, 8-oxogeranial, and methylvinylketone (MVK) (for chemical structures, see Supplemental Figure 1) were determined. Progesterone is a precursor in cardenolide biosynthesis (Gärtner et al., 1994; Kreis et al., 1998), whereas 2-cyclohexen-1-one was used as an alternative P5βR substrate in several studies (Munkert et al., 2011; Bauer et al., 2012). MVK, a small toxic molecule that can also be reduced by P5βR, was identified as a reactive electrophile that activates expression of defense genes and leads to a rise of jasmonate (JA) in *Arabidopsis* (Alméras et al., 2003). 8-Oxogeranial is the reported substrate for CrP5βR5/IS (Geu-Flores et al., 2012).

Gas chromatography (GC)–mass spectrometry (MS) analyses revealed that all available recombinant (r)CrP5βR enzymes reduced progesterone enantioselectively to 5β-pregane-3,20-dione and thus qualified as P5βRs *sensu stricto* (Supplemental Figure 2). Most of the rCrP5βRs enzymes tested were able to reduce most of the substrates, including 8-oxogeranial (Table 1). After incubation of rCrP5βR5/IS with 8-oxogeranial, iridodial was formed (Figure 4), reproducing the result of Geu-Flores et al. (2012). GC–MS and thin-layer chromatography analysis indicated that rCrP5βR1, rCrP5βR2, and rCrP5βR4 were also able to form iridodial from 8-oxogeranial (Figure 4). In the case of rCrP5βR6, only trace amounts of iridodial could be detected, hence it might also be capable of reducing 8-oxogeranial (Figure 4).

Next, enzymes were compared and classified using their catalytic efficacies (k_{cat}/K_M) as a measure. All kinetic constants were determined using a photometric assay for enzyme activity determination (Bauer et al., 2010). Apparent K_M, v_{max}, and k_{cat} values are shown in Table 1. 8-Oxogeranial was by far the best substrate for all rCrP5βRs (except rCrP5βR6, which was not further tested with this substrate). The efficacies were up to 1300 times higher than those for progesterone. For rCrP5βR5/IS with 8-oxogeranial as substrate, we determined K_M (8.8 μM) and k_{cat} (1.4/s) values very similar to those reported by Geu-Flores et al. (2012) (K_M, 4.5 μM; k_{cat}, 1.6/s; Table 1). rCrP5βR6 (cluster II) was more effective for progesterone than rCrP5βR2 or rCrP5βR4 of cluster I. Progesterone was only a very poor substrate for rCrP5βR5. Therefore, reliable kinetic constants could not be determined for this particular enzyme/substrate combination. Although considerable variation was detected among the rCrP5βR enzymes for the substrates 2-cyclohexen-1-one and MVK, a preference could be observed for both substrates with P5βRs from cluster I, in particular rCrP5βR2 (Table 1).

All Six CrP5βRs Are Localized in the Cytosol

The differences in substrate specificity can be interpreted as the evolution of different physiological functions for the different CrP5βRs *in planta* but, conversely, the overlap in substrate range may point to genetic redundancy. The actual substrate range *in planta* is also determined by the subcellular localization of the enzyme. To assess the subcellular localization of all CrP5βRs, *Nicotiana tabacum* Bright-Yellow-2 (BY-2) cells were co-transformed with constructs coding for green fluorescent protein (GFP)-tagged CrP5βR proteins and for free red fluorescent protein (RFP). Stable transgenic cultures emitting both red and green fluorescence were analyzed with confocal microscopy. The free RFP protein localized to the cytoplasm but was also present in the nucleus due to passive diffusion. The GFP signal of the GFP-CrP5βR5 fusion protein indicated a predominant cytosolic localization of CrP5βR5 (Figure 5A), which is in agreement with the previously reported localization of the protein in *C. roseus* cells (Geu-Flores et al., 2012). Likewise, all other CrP5βRs showed a localization pattern nearly identical to CrP5βR5, indicating a predominant cytosolic localization of all six CrP5βR enzymes (Figure 5B and 5C) and suggesting that at the subcellular level, all have potentially equal access to 8-oxogeranial.

Transcriptional Regulation of the *CrP5βRs*

Transcriptional regulation of gene expression is another regulatory level, if not the most important one, that determines the substrate range and specificity of the corresponding enzymes and eliminates apparent genetic redundancy. To investigate the transcriptional regulation of the *CrP5βRs*, we first analyzed their expression in the CathaCyc RNA-Seq atlas (Van Moerkercke et al., 2013; http://bioinformatics.psb.ugent.be/orcae/overview/Catro), which currently holds the expression data from the MPGR and SmartCell consortia and comprises a total of 30 different samples of different *C. roseus* plant organs, plants, suspension cells, and hairy roots under various conditions. A cluster analysis with all known MIA biosynthesis genes (Courdavault et al., 2014; Miettinen et al., 2014) confirmed the tight co-regulation of *CrP5βR5/IS* with the other early genes of
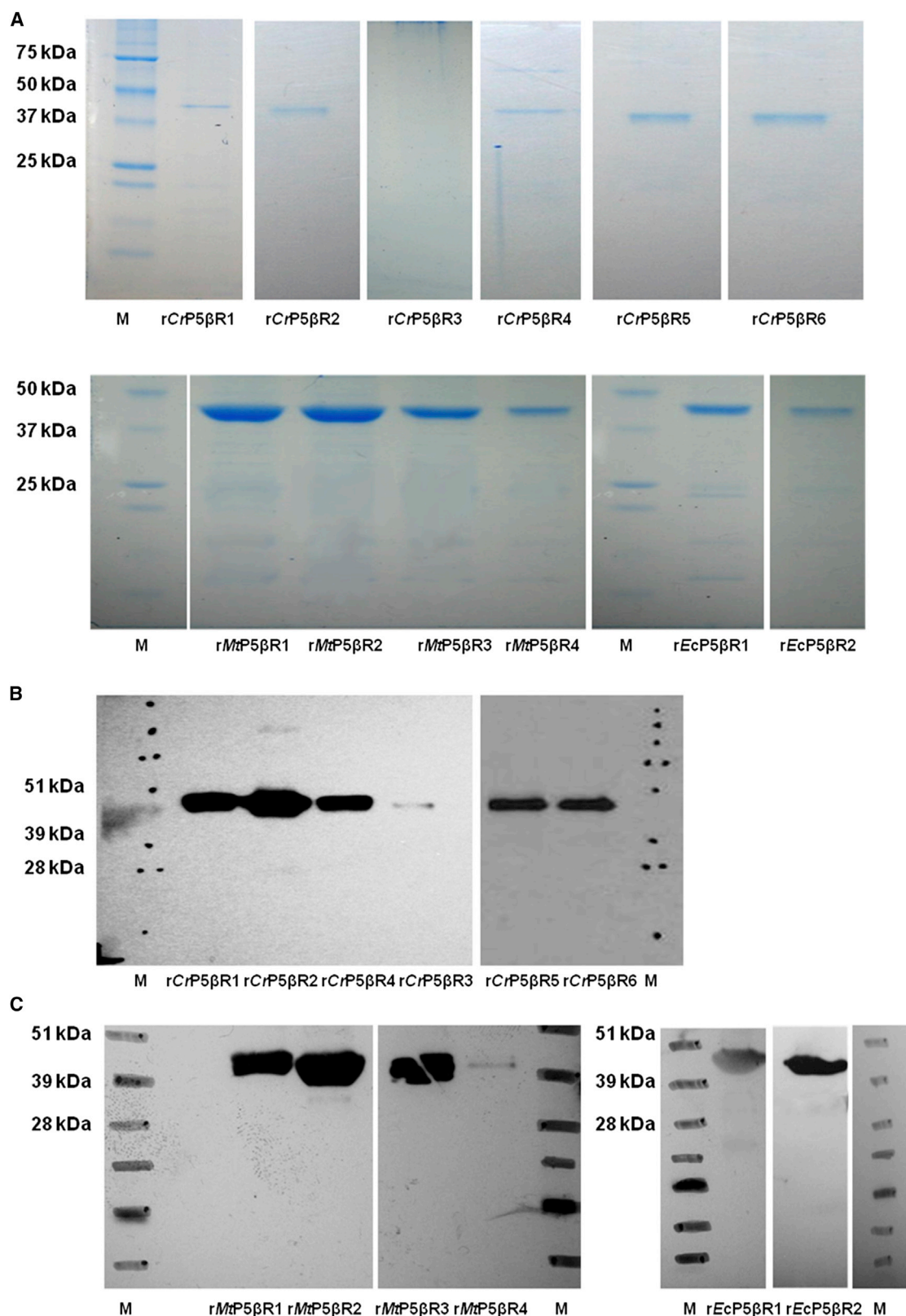
Figure 3. SDS–PAGE and Immunoblot Analyses of rCrP5βR, rMtP5βR, and rEcP5βR Proteins.

(A) SDS–PAGE analysis of recombinant CrP5βRs, MtP5βRs, and EcP5βRs. Purified rP5βR proteins have a size of about 42 kDa and were visualized with Coomassie-Brilliant-Blue R 250. For rAtVEP1, see Herl et al. (2009).

(B and C) Immunoblot analysis of rCrP5βRs **(B)**, MtP5βRs and EcP5βRs **(C)** using anti-His antibodies (primary) and anti-mouse IgG-peroxidase antibodies (secondary). Chemiluminescence was used for detection. For rAtVEP1, see Herl et al. (2009).

Enzyme	Substrate											
	Progesterone			**Cyclohexen-1-one**			**8-Oxogeranial**			**MVK**		
	K_M (µM)	k_{cat} (s^{-1})	k_{cat}/K_M (s^{-1} M^{-1})	K_M (µM)	k_{cat} (s^{-1})	k_{cat}/K_M (s^{-1} M^{-1})	K_M (µM)	k_{cat} (s^{-1})	k_{cat}/K_M (s^{-1} M^{-1})	K_M (µM)	k_{cat} (s^{-1})	k_{cat}/K_M (s^{-1} M^{-1})
P5βRs from Cluster I (see Figure 2)												
rCrP5βR1	n.i.			n.i.			8.9	1.15	128 940	n.i.		
rCrP5βR2	100	0.02	232.7	115.8	0.86	7426	10.1	1.22	120 731	148	0.86	5829
rCrP5βR4	153	0.019	123	296	0.03	104	7.8	0.96	122 569	123	0.20	1562
rEcP5βR1	77	0.01	130*	518	2.45	4730*	20	1.18	56 663	344	0.73	2143
rMtP5βR1	144	0.50	3652	82.1	0.32	5321	9.3	0.91	97 780	136	0.54	3992
rMtP5βR2	73	0.40	5631	214	0.04	220	11.7	0.76	64 889	111	0.08	701
P5βRs from Cluster II (see Figure 2)												
rCrP5βR5	n.i.			231	0.01	43	8.8	1.4	155 560	110	0.04	364
rCrP5βR6	75.5	0.40	5530	128	0.03	233	n.d.			118	0.03	261
rEcP5βR2	82	0.045	552	325	0.007	20	n.d.			224	0.05	245
rMtP5βR3	260	0.04	154	109	0.017	155	n.d.			86.7	0.02	201
rMtP5βR4	n.i.			136	0.006	46	n.d.			89.9	0.016	185

Table 1. Kinetic Data of Different P5βRs from *Catharanthus roseus*, *Medicago truncatula*, and *Erysimum crepidifolium*.

SD K_M ± ≤25%; n.i., not investigated; n.d., no *cis-trans* iridoidal was detected as product.
*Munkert et al. (2011).

the iridoid pathway, such as *geraniol synthase* (*GES*), *geraniol 8-oxidase* (*G8O*), and *8-hydroxygeraniol oxidoreductase* (*8-HGO*) (Figure 6).

These four, as well as almost all other known MIA genes, were induced by methyl jasmonate (MeJA), both in cell suspension cultures and whole *C. roseus* plants (Figure 6; Supplemental Table 1). Nonetheless, the early iridoid pathway genes, such as *CrP5βR5/IS* on the one hand, and the late iridoid and downstream MIA genes, such as *loganic acid O-methyltransferase* (*LAMT*), *secologanin synthase* (*SLS*), *strictosidine synthase* (*STR*), and *strictosidine β-glucosidase* (*SGD*) on the other hand, showed different induction characteristics and grouped in two distinct expression clusters (Figure 6). *CrP5βR4* grouped in the *SLS/STR* cluster. In contrast to the *STR* gene, however, which is a known target of the transcriptional regulator ORCA3 (van der Fits and Memelink, 2000), *CrP5βR4* expression was not elevated in the *ORCA3* overexpressing cell suspension cultures. This was similar to *CrP5βR5/IS*, but also to other iridoid genes acting downstream of *CrP5βR5/IS* but before *LAMT*, and including *iridoid oxidase* (*IO*), *7-deoxyloganetic acid glucosyl transferase* (*7-DLGT*) and *7-deoxyloganic acid hydroxylase* (*7-DLH*), which also grouped in the *SLS/STR* cluster in our analysis (Figure 6; Supplemental Table 1). Overall, this supports a possible link with secoiridoid biosynthesis for *CrP5βR4.*

In contrast, the *CrP5βR1*, *CrP5βR2*, *CrP5βR3*, and *CrP5βR6* genes were not inducible by MeJA and did not cluster with the known iridoid or MIA genes (Figure 6; Supplemental Table 1). In fact, *CrP5βR1*, *CrP5βR3*, and *CrP5βR6* were hardly expressed and had constitutive low levels across all samples analyzed (Figure 6; Supplemental Table 2). *CrP5βR2* also had a constitutive expression across all transcriptome samples, but

showed higher absolute transcript counts (Figure 6; Supplemental Table 2).

### Transcripts of *CrP5βR4* Colocalize with Those of *CrP5βR5* in the IPAP Cells

The multicellular nature of the MIA biosynthetic pathway in *C. roseus* is well known, with the biosynthesis taking place in at least four different cell types. The early steps of the biosynthesis, from the MEP pathway up to the synthesis of loganic acid, take place in the internal phloem-associated parenchyma (IPAP) cells. The subsequent steps of the pathway take place in the epidermis, ending ultimately in laticifers and idioblasts, specialized alkaloid-accumulating cells (Courdavault et al., 2014).

Correspondingly, it was reported that the transcripts of *CrP5βR5/IS* localize in the IPAP cells (Geu-Flores et al., 2012), as well as those of the early part of the secoiridoid pathway up to 7-deoxyloganic acid hydroxylase (7-DLH; Miettinen et al., 2014). Conversely, transcripts corresponding to the subsequent steps, such as *SLS*, *STR*, and *SGD*, localize in the epidermis (St-Pierre et al., 1999; Courdavault et al., 2014).

To further assess their possible involvement in iridoid synthesis, the localization of all *CrP5βR* transcripts was investigated by RNA *in situ* hybridization performed on cross-sectioned apical parts of the plant, i.e., young developing leaves and flower buds. Using antisense probes, the transcripts of *CrP5βR4* and *CrP5βR5* were shown to localize in the IPAP cells of all developing aerial organs (Figure 7). As positive controls, antisense probes for *G8O* and *SGD* transcripts, which localize to the IPAP and epidermis cells, respectively (Burlat et al., 2004), were used (Figure 7). No signals were detected with the *CrP5βR4* and *CrP5βR5* sense probes used as negative controls. No signals
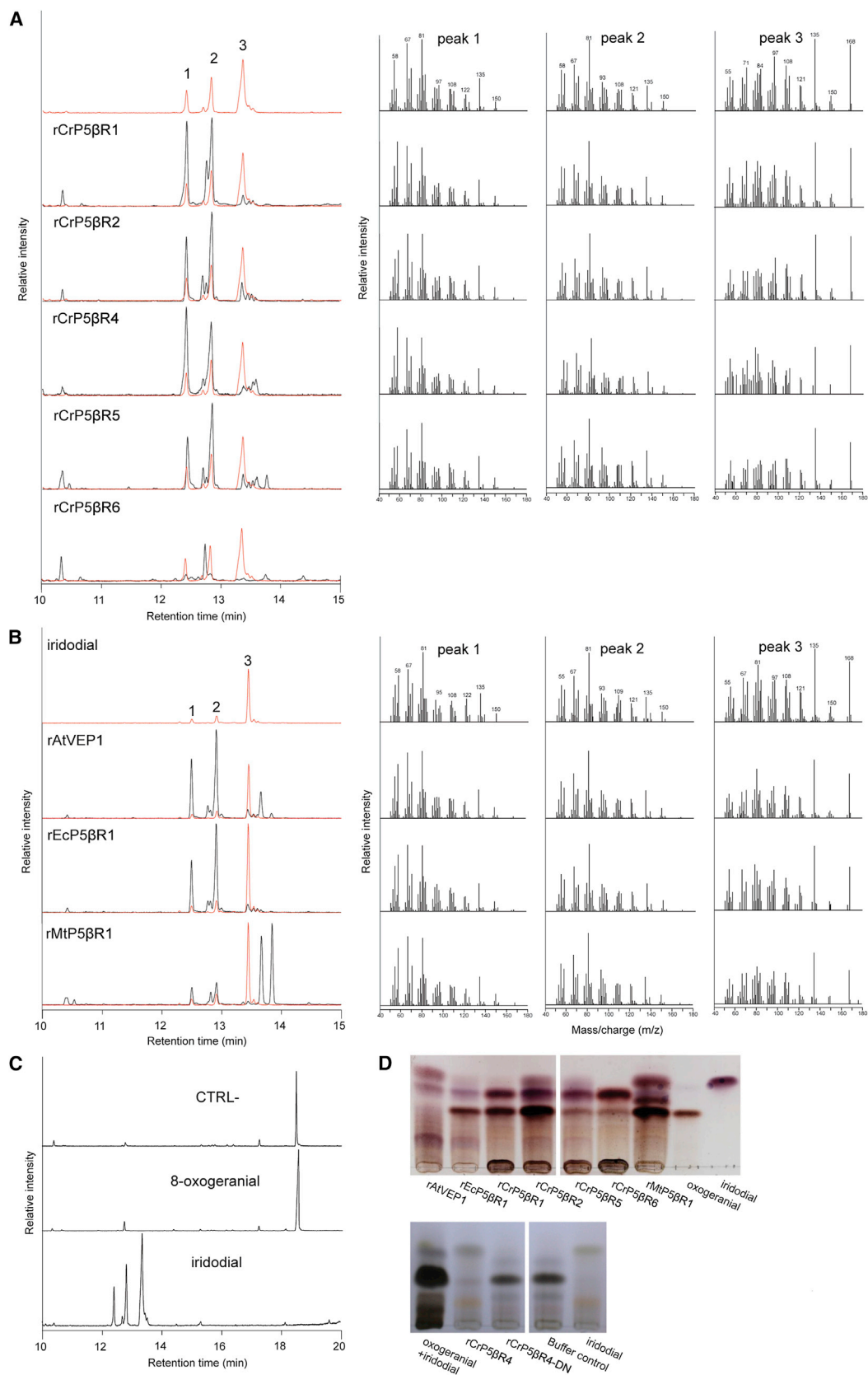
(legend on next page)
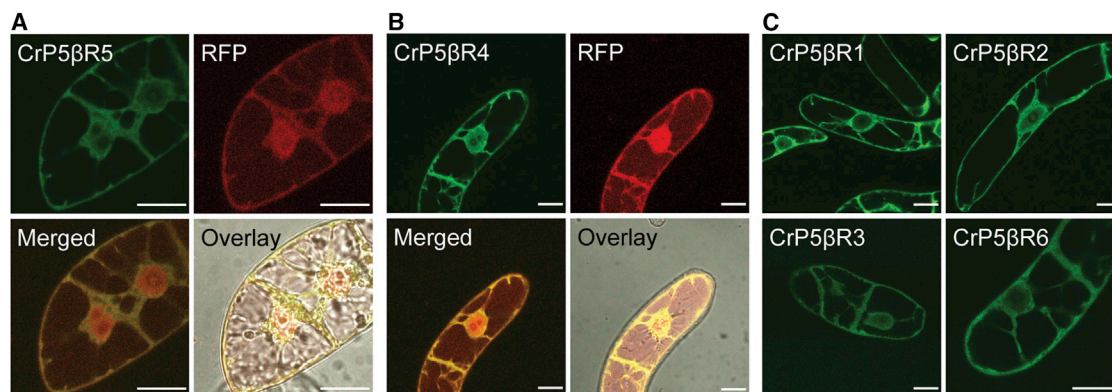
Figure 5. Localization of the Six CrP5βRs in BY-2 Cells.

(A and B) Confocal microscopy analysis of BY-2 cells co-transformed with a GFP-CrP5βR5 (**A**, top left) or a GFP-CrP5βR4 (**B**, top left) construct and a free RFP (**A** and **B**, top right) construct.

(C) Confocal microscopy analysis of BY-2 cells transformed with a GFP-CrP5βR1 (top left), CrP5βR2 (top right), CrP5βR3 (bottom left), CrP5βR6 (bottom right) construct. Scale bars, 20 μm.

were detected with the probes for the other *CrP5βR*s, which is likely due to the low transcript abundance in the tissues investigated (Supplemental Table 2). These data suggest that both *CrP5βR4* and *CrP5βR5* may be involved, redundantly or not, in MIA biosynthesis in *C. roseus* within the same aerial organs.

In Planta Silencing of *CrP5βR2* and *CrP5βR4*

To investigate whether CrP5βR4 contributes to iridoid synthesis *in planta*, we used virus-induced gene silencing (VIGS) to down-regulate *CrP5βR4* in young *C. roseus* leaves. The *CrP5βR5/IS* that was previously studied (Geu-Flores et al., 2012) was also tested in this system. Because *CrP5βR1*, *CrP5βR3*, and *CrP5βR6* transcripts were hardly or not detectable in *C. roseus* (Supplemental Tables 1 and 2), they were not considered for VIGS experiments. In contrast, although *CrP5βR2* transcripts were not detectable by *in situ* hybridization (ISH) and were not MeJA inducible, a VIGS construct was also designed for *CrP5βR2*, because transcripts of *CrP5βR2* in *C. roseus* leaves showed absolute counts that were about half those of *CrP5βR4* and *CrP5βR5/IS* (Supplemental Tables 1 and 2).

Quantitative real-time PCR (qRT–PCR) demonstrated that all VIGS constructs efficiently silenced the target *CrP5βR* gene(s) within 25 days after infection (Figure 8A–8C). As in Geu-Flores et al. (2012), we observed a significant and specific increase in the accumulation of three abundant putative iridoid peaks that

appear to be derived from the *CrP5βR* substrate 8-oxogeranial (*m/z* 526, 528, and 484; Figure 8E). In contrast to the previous study, we did not observe a significant difference in strictosidine and vindoline in the *CrP5βR5/IS* silenced lines (Figure 8D). A possible explanation could be the use of different *C. roseus* cultivars: Geu-Flores et al. (2012) used Little Bright Eye; we used Sunstorm Rose, which has lower levels of vindoline and other MIAs, but which became the preferred cultivar for VIGS because of its superior reproducibility due to more homogeneous growth rates. Alternatively, we used a different region of the gene for silencing, and this may affect the chemotype. Since *CrP5βR5/IS* silenced lines did show a significant and specific increase in the accumulation of three of the most abundant unidentified putative iridoid peaks (*m/z* 526, 528, and 484; Figure 8E), which were also specifically detected in the *CrP5βR5/IS* silenced lines in the study of Geu-Flores et al. (2012), this confirms the involvement of *CrP5βR5/IS* in secoiridoid biosynthesis also in the Sunstorm Rose cultivar, as well as the reliability of our experiment.

No significant differences in the vindoline and strictosidine peaks could be detected for any of the *CrP5βR2* or *CrP5βR4* silenced lines in comparison to the empty vector control, nor could any of the putative iridoid peaks be spotted that accumulate in the *CrP5βR5/IS* silenced lines (Figure 8E), suggesting that CrP5βR2 and/or CrP5βR4 do not contribute to secoiridoid synthesis *in planta*, at least not when CrP5βR5/IS is present.

**Figure 4. Multiple rP5βR Proteins Convert 8-Oxogeranial to Iridodial.**

(A) Overlay of GC chromatograms (left panels) of the reaction products of rCrP5βR proteins incubated with the substrate 8-oxogeranial (black) and an authentic *cis-trans* iridodial standard (red). Representative electron ionization–MS spectra (right panels) of the rCrP5βR reaction products. The spectrum is identical to the *cis-trans* iridodial authentic standard. For rCrP5βR6, no informative electron ionization–MS spectra could be included since only trace amounts of iridodial accumulated.

(B) Overlay of GC chromatograms of the reaction products of rAtVEP1, rEcP5βR, and rMtP5βR proteins incubated with the substrate 8-oxogeranial (black) and an authentic *cis-trans* iridodial standard (red).

(C) GC chromatogram of a control experiment showing a lack of conversion of 8-oxogeranial to *cis-trans* iridodial in the presence of denatured rCrP5βR proteins (CTRL–).

(D) Thin-layer chromatography of the reaction products from different rP5βR proteins with 8-oxogeranial as substrate. rCrP5βR4-DN, denatured rCrP5βR4.
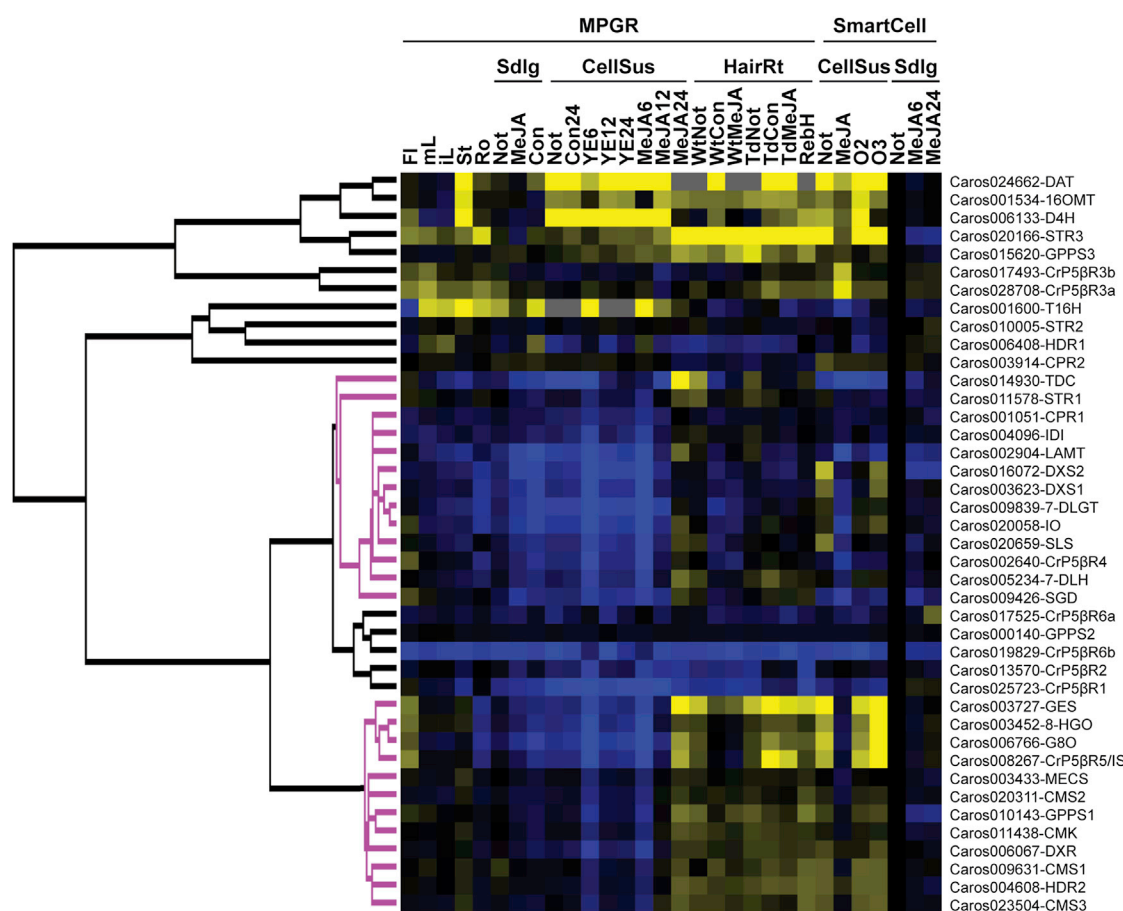
Figure 6. *CrP5βR4* Is Co-expressed with Secoiridoid Pathway Genes.
Average linkage hierarchical clustering of early MIA pathway gene expression in *C. roseus* based on the RNA-Seq data from the SmartCell (http://bioinformatics.psb.ugent.be/orcae/overview/Catro) and the Medicinal Plant Genomics Resource (MPGR) (http://medicinalplantgenomics.msu.edu) consortia. Colors indicate transcriptional induction (blue) or repression (yellow) relative to untreated seedling samples from SmartCell (Not). Upper and lower pink-colored tree branches correspond to the *CrP5βR4* and *CrP5βR5* containing clusters, respectively. Tissues: Fl, flower; mL, mature leaves; iL, immature leaves; St, stem; Ro, root. Sdlg, seedling. CellSus, Suspension cells: O2, ORCA2; O3, ORCA3. HairRt, hairy roots: Wt, wild-type; Td, TDCi; RebH, RebH_F. Treatments: Not, no treatment; MeJA, methyl jasmonate (6, 12, or 24 h); Con, mock; YE, yeast extract. Enzymes: CMK, 4-(cytidine 50-diphospho)-2C-methyl-D-erythritol kinase; CMS, 4-(cytidine 50-diphospho)-2C-methyl-D-erythritol synthase; CPR, cytochrome P450 reductase; DAT, deacetylvindoline 4-O-acetyltransferase; D4H, desacetoxyvindoline 4-hydroxylase; 7-DLGT, 7-deoxyloganetic acid glucosyl transferase; 7-DLH, 7-deoxyloganic acid hydroxylase; DXS, 1-deoxy-D-xylulose-5-phosphate synthase; DXR, 1-deoxy-D-xylulose-5-phosphate reductoisomerase; GES, geraniol synthase; G8O, geraniol 8-oxidase; GPPS, geranyl diphosphate synthase; HDR, hydroxymethylbutenyl 4-diphosphate reductase; 8-HGO, 8-hydroxygeraniol oxidoreductase; IDI, isopentenyl diphosphate isomerase; IO, iridoid oxidase; IS, iridoid synthase; LAMT, loganic acid O-methyltransferase; MECS, 2C-methyl-D-erythritol-2,4-cyclodiphosphate synthase; 16OMT, 16-hydroxytabersonine O-methyltransferase; SGD, strictosidine β-glucosidase; SLS, secologanin synthase; STR, strictosidine synthase; TDC, tryptophan decarboxylase; T16H, tabersonine 16-hydroxylase.

In agreement with previous reports (Asada et al., 2013; Salim et al., 2013), we could not reliably detect other secoiridoid intermediates, such as 7-deoxyloganic acid and loganic acid, in wild-type or empty vector (non-silenced) control *C. roseus* leaves. Hence, we were not able to assess possible decreases in the intensity of these compounds in leaves silenced for *CrP5BR4* or *CrP5BR5*.

rP5βRs from Other Plant Species Can Also Use 8-Oxogeranial as a Substrate

To test whether only CrP5βRs take 8-oxogeranial as a substrate, we cloned *P5βR* genes from a number of other plant species, such as *Medicago truncatula* (*MtP5βR1* to *MtP5βR4*),

E. crepidifolium (*EcP5βR1* and *EcP5βR2*), and *Arabidopsis* (*AtVEP1*; Herl et al., 2009), and produced the corresponding recombinant proteins in *E. coli* and tested their activities and kinetic constants with the same substrates as for the CrP5βRs.

The rMtP5βRs, rEcP5βRs, and rAtVEP1 were also able to reduce all substrates, including 8-oxogeranial, indicating that this is an intrinsic substrate for rP5βRs of angiosperm species (Figure 4; Table 1). Remarkably, 8-oxogeranial was even the best substrate for all rP5βRs investigated here. When progesterone was used as substrate, rEcP5βR2 of cluster II had a higher efficacy than rEcP5βR1 of cluster I (Table 1), similar to the situation for the rCrP5βR cluster I and II enzymes. Likewise, the rDpP5βR2 of *Digitalis purpurea* also had a higher progesterone affinity than

Figure 7. Co-expression of *CrP5βR4* and *CrP5βR5/IS* in the Internal Phloem-Associated Parenchyma (IPAP) Cells.

In situ hybridization on serial cross sections of young developing leaves (left columns) and flower buds (taken here at the petal level; right columns) was carried out with antisense (AS) probes, and as controls with sense (S) probes. Geraniol 8-oxidase (G8O) and strictosidine β-D-glucosidase (SGD) AS probes were used as IPAP and epidermis markers, respectively. Sense probe controls gave no signals. ep, epidermis; IPAP, internal phloem-associated parenchyma. The IPAP signal was also detected in other flower bud parts (stamen, sepals, carpels) for *CrP5βR4* and *CrP5βR5/IS* (data not shown). Scale bar, 100 μm.

its rDpP5βR cluster I paralog (Pérez-Bermúdez et al., 2010). However, for the *M. truncatula* rP5βRs it was vice versa. The efficacies of rMtP5βR1 and rMtP5βR2 (both cluster I) for progesterone were about 10–50 times higher than those of the cluster II MtP5βRs (Table 1).

rP5βRs from clusters I and II could be discriminated in their preferences for the substrates 2-cyclohexen-1-one and MVK. For the

substrate 2-cyclohexen-1-one, a preference with P5βRs from cluster I could be detected (e.g., rEcP5βR1, rMtP5βR1, or rCrP5βR2). MVK was also accepted as a substrate by all P5βRs. Again, considerable variation was seen among the enzymes characterized and preferences with P5βRs from cluster I were observed. For rEcP5βR1, rMtP5βR1, rCrP5βR2, or rCrP5βR4, we could determine turnover rates between 0.5 and 0.87/s for MVK, whereas k_{cat} values measured for rEcP5βR2 or
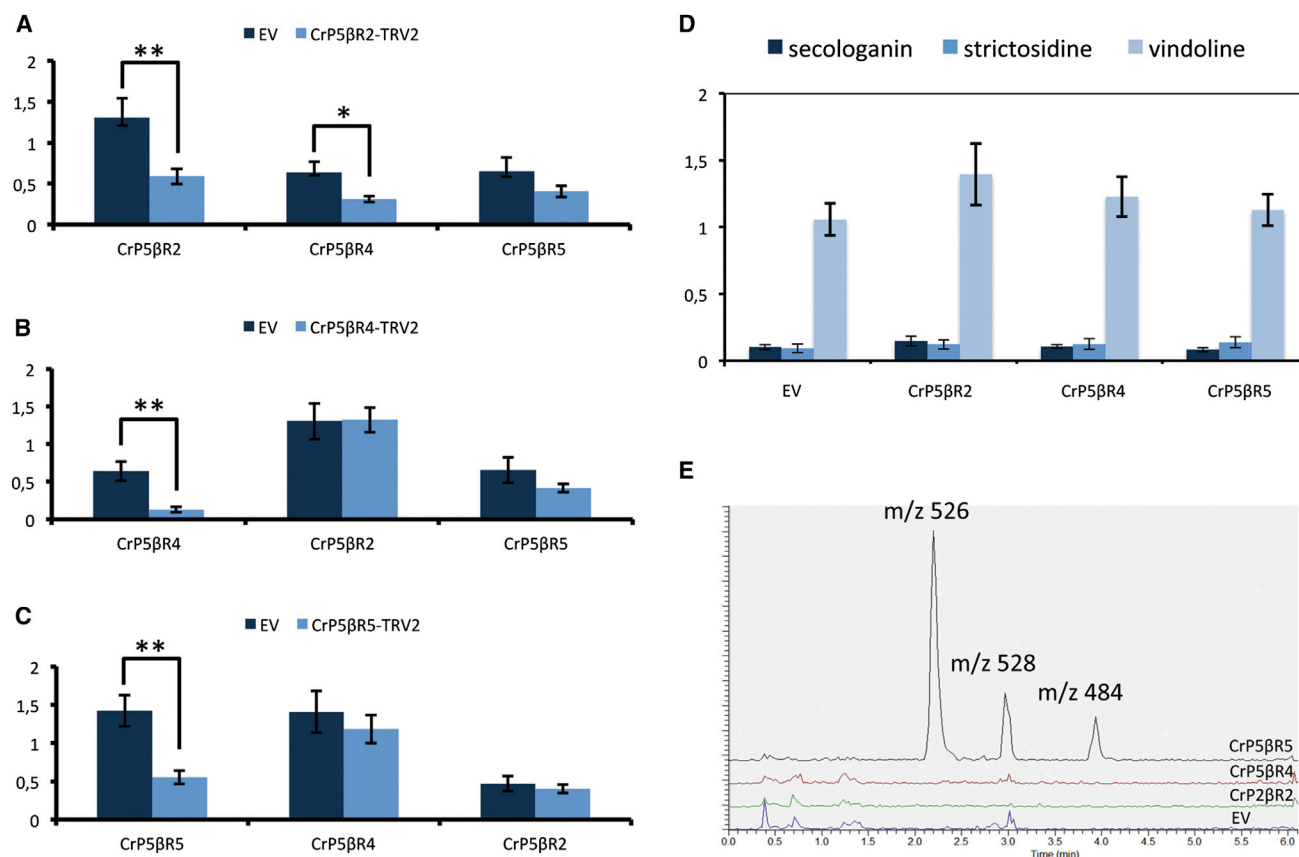
Figure 8. Assessment of the *In Planta* Role of *CrP5βR* Genes in Secoiridoid and Monoterpenoid Indole Alkaloid (MIA) Biosynthesis by Virus-Induced Silencing (VIGS) in *C. roseus* Leaves.

(A–C) Effect on transcript accumulation in lines silenced for *CrP5βR2* **(A)**, *CrP5βR4* **(B)**, and *CrP5βR5* **(C)**. The *y* axis denotes the normalized relative transcript accumulation of the *CrP5βR* genes indicated in the *x* axis. Standard errors are shown ($n = 7$ for EV and $n = 10$ for *CrP5βR*; Student's *t*-test, *$P > 0.05$, **$P > 0.005$). EV, empty vector.

(D) Quantification of the major secoiridoids and MIAs by liquid chromatography–MS. EV, empty vector control. The *y* axis denotes the normalized intensity (peak area/leaf mass $\times 10^{10}$). Asterisks denote statistical significance ($P < 0.05$ on unpaired Student's *t*-tests). Error bars represent standard errors.

(E) Extracted ion chromatograms for *m/z* 526, 528, 484 in lines silenced for the different *CrP5βR* genes.

rCrP5βR6 and other rP5βRs of cluster II were only between 0.016 and 0.05/s (Table 1).

Modeling of the Binding Pocket of the CrP5βR Proteins

P5βRs are members of the large SDR superfamily of enzymes (Jörnvall et al., 1995). They all belong to the new class of SDRs characterized by Thorn et al. (2008). They can be classified as stereoselective enone-reductases capable of reducing activated C = C double bonds by a 1,4-addition mechanism. A hydride is transferred from NADPH to a carbonyl-activated double bond and the carbonyl is then protonated. An enol intermediate is formed, which tautomerizes to the final product (Thorn et al., 2008). Besides the two important amino acids in the catalytic site (K147 and Y179), five additional amino acids are highly conserved in the binding pocket. These amino acids are W106, G145, F153, M215, and F343 (Bauer et al., 2010; Supplemental Table 3). Here, we modeled the active sites and amino acid residues of the substrate binding site using DIP5βR (Protein Data Bank ID 2V6G) with progesterone docked in the catalytic site as a template (Figure 9). As far as the binding pocket is concerned, homology modeling using 2V6G as the template

revealed the high similarity between DIP5βR, CrP5βR1, and CrP5βR2. This structural feature coincides with very similar turnover rates for progesterone (ca. 0.02/s; Bauer et al., 2012; Figure 9A–9C). Furthermore, there is also a difference in the orientation of phenylalanine-343 in CrP5βR4. It is turned about 180° outward of the binding pocket. Because phenylalanine-153 and phenylalanine-343 normally work together as a clamp for the binding and holding of the substrate in the binding pocket, this different orientation of the CrP5βR4 phenylalanine-343 could be a reason for the lower turnover rate of the corresponding recombinant enzyme, especially with small substrates, such as MVK or 2-cyclohexen-1-one, compared to the efficacy of rCrP5βR2 (about 5–25 times less; Figure 9D). For rCrP5βR5, only a very low activity for progesterone was measured. A 180° rotation of the tryptophan in CrP5βR5 (W109) was observed (Figure 9E). With a distance of more than 5 Å, it is hardly possible to be involved in binding progesterone in the binding pocket. Because this different position of the tryptophan has no effect on the activity toward the other substrates tested, it seems to be only necessary for the binding of progesterone. Since CrP5βR6 (cluster II) belongs to a different phylogenetic cluster of P5βRs compared to DIP5βR1, CrP5βR1, or CrP5βR2,

many structure differences were seen (Figure 9F). The changes from phenylalanine-153 of DIP5βR1 to isoleucine-138 of CrP5βR6 and phenylalanine-343 of DIP5βR1 to alanine-328 of CrP5βR6 are especially interesting and may be responsible for a higher activity toward progesterone. Essential for this increased activity could be an improvement in the orientation of progesterone, because of the higher flexibility of small, but also hydrophobic, amino acids and of a second tyrosine (Y200/Figure 9F), which is located close to the substrate and might be beneficial for catalytic activity.

DISCUSSION

Plant-specialized metabolism is characterized by a huge diversity of chemical structures that play important roles in growth, development, or interaction with the environment. The plant kingdom is estimated to be able to synthesize over 100 000 different specialized metabolites. The evolution of the respective, often species-specific, biosynthetic pathways has required the evolution of new genes, for instance encoding enzymes and transporters, as well as new regulatory networks. Gene duplications with successive diversifications are a central mechanism in evolution and are regarded as the major driving force in the generation of the evolutionary variety in plant-specialized metabolism (Ober, 2010).

The *C. roseus* P5βR Family, Redundant or Not?

In this study, this evolutionary principle is further illustrated. Previously, one P5βR homolog, i.e., IS or CrP5βR5, was isolated from *C. roseus* and shown to catalyze the reduction of 8-oxogeranial to iridodial in the secoiridoid branch of the MIA biosynthetic pathway (Geu-Flores et al., 2012). Here, through mining of transcriptome data, we identified five new members of the *C. roseus* P5βR family, denominated CrP5βR1 to CrP5βR4 and CrP5βR6. Biochemical characterization of rCrP5βR proteins demonstrated that, besides rCrP5βR5/IS, rCrP5βR1, rCRP5βR2, and rCrP5βR4 can also convert 8-oxogeranial to iridodial, indicating that potentially multiple CrP5βR proteins could be involved in secoiridoid biosynthesis in *C. roseus*.

To assess the above postulation, we investigated the expression, localization, and activity of the CrP5βR proteins *in planta*. The actual substrate pool of an enzyme, and thus its activity *in planta*, is determined by its subcellular localization and that of its substrates. Modifications in this feature can be an important driver of the evolution of novel biosynthetic pathways, which has for instance been nicely illustrated for the biosynthesis of the anti-malarial sesquiterpenoid artemisinin in the medicinal plant *Artemisia annua*, involving the enzyme DBR2, which reduces the Δ11(13) double bond originating in amorpha-4,11-diene (Zhang et al., 2008). DBR2 is a member of the enoate reductase family to which the ubiquitous peroxisomal 12-oxophytodienoate reductases (OPRs), involved in JA biosynthesis, also belong. An evolutionary mutation in DBR2, disrupting the Ser-Arg-Leu tripeptide peroxisomal targeting signal, caused DBR2 to accumulate exclusively in the cytosol, allowing it to be recruited to the artemisinin biosynthetic pathway that depends on cytosolic sesquiterpenoid precursors (Zhang et al., 2008). In the case of the CrP5βR proteins, all showed a predominant cytosolic localization, similar to the CrP5βR5/IS enzyme itself, suggesting they can theoretically

encounter 8-oxogeranial as a substrate at the subcellular level (Courdavault et al., 2014) and thus be involved in secoiridoid biosynthesis.

Transcriptional regulation is another level that determines substrate pool and specificity. In the case of secoiridoid biosynthesis in *C. roseus*, two important transcriptional regulatory levels exist. The first is the responsiveness to particular phytohormones and environmental signals and the second is the tissue specificity. All secoiridoid genes are responsive to (Me)JA, but display two distinct cellular expression patterns. Transcripts corresponding to the early enzymes in the pathway, up to 7-DLH and comprising CrP5βR5/IS, localize in the IPAP cells, whereas those corresponding to the subsequent steps of the pathway localize in the epidermis (St-Pierre et al., 1999; Geu-Flores et al., 2012; Courdavault et al., 2014; Miettinen et al., 2014). Expression analysis of all *CrP5βR*s indicated that only one other member of the *CrP5βR* family besides *IS/CrP5βR5*, namely *CrP5βR4*, was responsive to MeJA, and could be detected in the IPAP cells, thus limiting possible genetic redundancy between the *CrP5βR* family members in secoiridoid biosynthesis to two. VIGS analysis was not conclusive in resolving this issue, however. It suggested that in the presence of CrP5βR5/IS, CrP5βR4 contributes little or nothing to secoiridoid and MIA biosynthesis *in planta*, but nonetheless, a role for CrP5βR4 in this pathway, perhaps in particular conditions or tissues, could not be entirely ruled out yet.

CrP5βR1, *CrP5βR3*, and *CrP5βR6* were hardly expressed, as illustrated by the constitutive low levels across all RNA-Seq samples and the absence of detectable signals in the ISH analysis, and were thus not included in the VIGS experiments. In contrast, *CrP5βR2* also showed constitutive expression across all transcriptome samples, but with higher absolute transcript levels than *CrP5βR1*, *CrP5βR3*, and *CrP5βR6*, but still about two-fold lower than *CrP5βR4* and *CrP5βR5/IS*. Nonetheless, *CrP5βR2* transcripts could not be detected by ISH in either *C. roseus* leaves or flowers, which may point to ubiquitous or a less pronounced cell-specific expression and at least excluding IPAP-specific expression. Accordingly, VIGS analysis did not support a role for CrP5βR2 in secoiridoid production *in planta*.

Can All Angiosperm P5βRs Catalyze 8-Oxogeranial Reduction to Iridodial?

P5βRs were termed as such because they convert progesterone to 5β-pregnane-3,20-dione enantioselectively. *P5βR* genes have first been identified in cardenolide-producing plant species, such as *D. lanata* and *E. crepidifolium*, but also in cardenolide-free plants of the angiosperm lineage, such as the model plant *Arabidopsis*. Most angiosperm species have several P5βRs encoded in their genome, and hitherto, all recombinant P5βR enzymes tested have been found capable of reducing a large variety of substrates bearing an active C = C double bond by an 1,4-addition mechanism using NADPH as the co-substrate (Gärtner et al., 1994; Burda et al., 2009; Bauer et al., 2010). Accordingly, all rCrP5βR proteins, except for rCrP5βR3, which we were unable to produce as a recombinant protein, could reduce several substrates, such as progesterone and 2-cyclohexen-1-one, using NADPH as the co-substrate, and can thus be qualified as genuine P5βRs.
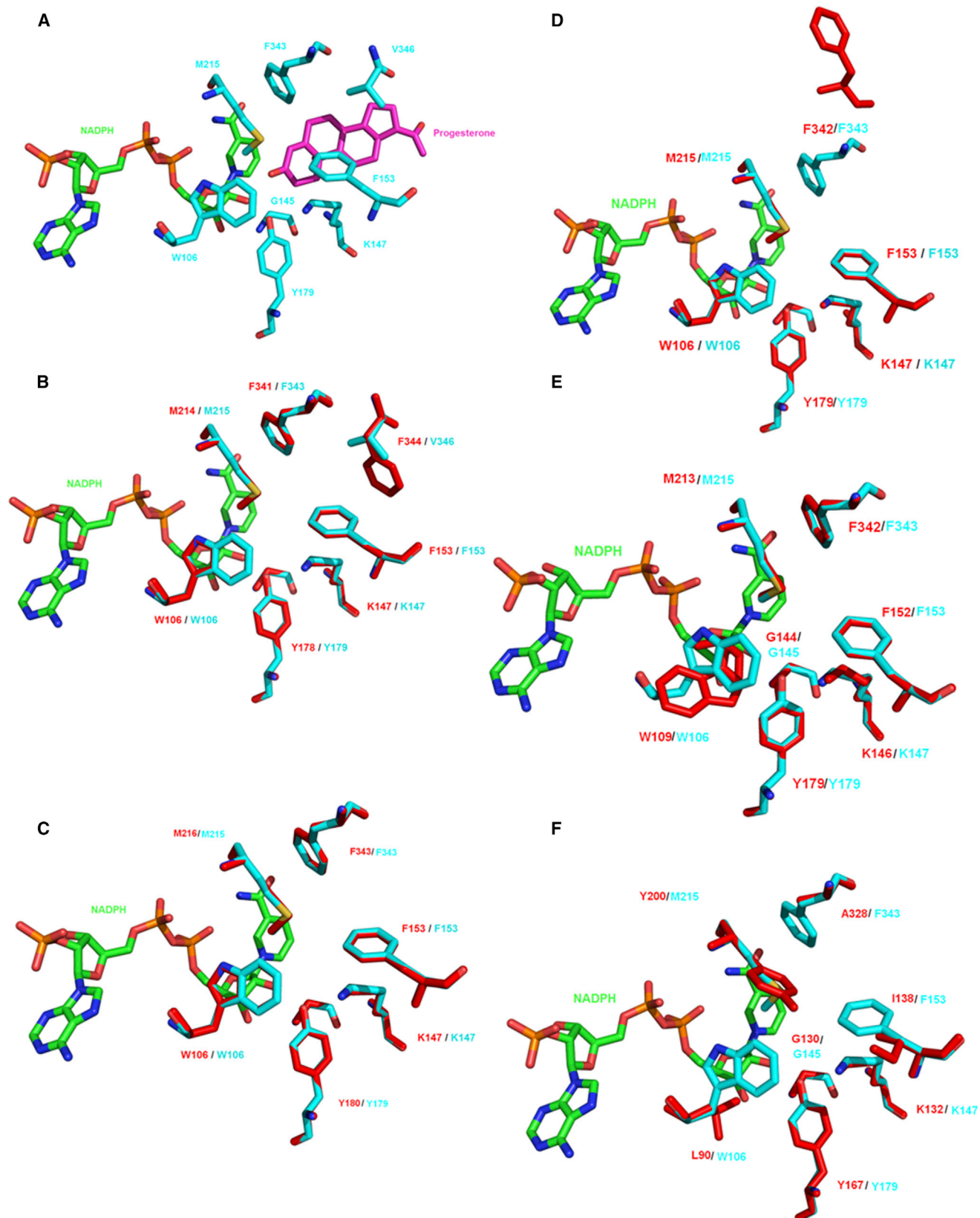
(legend on next page)

The fact that 8-oxogeranial can be taken as a substrate by nearly all CrP5βRs from both subclades raised the question whether this is an intrinsic capacity of other angiosperm P5βRs, or whether it is specific for the P5βRs from iridoid-producing plant species. Cloning and characterization of P5βRs from two other plant species that encode several P5βRs in their genome, i.e., the cardenolide- and iridoid-free model plants *M. truncatula* and *Arabidopsis*, and the iridoid-free but cardenolide-producing *E. crepidifolium*, demonstrated that nearly all rP5βRs tested were capable of taking 8-oxogeranial as a substrate. This suggests that IS activity is indeed an intrinsic capacity of angiosperm P5βR proteins, which might have evolved early during evolution.

The wide substrate range can be interpreted as the evolution of different physiological functions for different P5βRs *in planta*. Besides the already elucidated role in iridoid and cardenolide biosynthesis, a role in the detoxification of small toxic molecules, such as MVK, is also plausible. Further interesting substrates for verifying this hypothesis, such as 2(*E*)-hexenal, traumatine or 2(*E*)-nonenal (Alméras et al., 2003), have not been tested yet with the P5βRs identified here. Taking into account the occurrence of several paralogous *P5βR* genes in a single plant species and the substrate promiscuity of the enzymes, it is possible that P5βRs are responsible for different functions within the same plant. Substrate-promiscuous enzymes sustain the formation of high numbers of small natural products that provide its producer with a selective advantage in an evolutionary context. Similarly, such enzymes might provide a selective advantage because of increased detoxification capacities for the organism.

The relaxed substrate specificity of angiosperm P5βRs clearly underscores their capacity to be involved or become recruited in more biosynthetic pathways than currently known. P5βRs have a wide occurrence within the angiosperm lineage (Bauer et al., 2010), and over 100 angiosperm *P5βR* genes can currently be found in the NCBI database. It will be interesting to find out how many P5βRs, and from which species, eventually became recruited to specialized metabolic pathways, such as that of iridoid biosynthesis. Conversely, our findings might raise the question whether iridoid biosynthesis might be more widespread than currently assumed and may still be undiscovered in some plant species, for instance because of a highly cell-specific expression?

METHODS

Gene Isolation

All gene products were PCR amplified for Gateway (Invitrogen) cloning from a cDNA template of *C. roseus*, *M. truncatula*, or *E. crepidifolium* using the primer pairs shown in Supplemental Table 4.

For standard PCR, the following amplification program was used: 30 s at 98°C; 7 cycles of 10 s denaturation at 98°C, followed by 30 s annealing at 42°C, and 90 s extension at 72°C; 23 cycles of 10 s denaturation at 98°C, followed by 30 s annealing at 56°C and 90 s extension at 72°C; 5 min extension at 72°C. Amplified fragments of a size of ca. 1200 bp were cut out from a 1% agarose gel and were purified with the Fermentas GeneJET Gel Extraction Kit. Purified PCR fragments were introduced into pDONR221 and then transferred to the pDEST17 vector by Gateway recombination. *E. coli* BL21 (DE3) cells, transformed with the pDEST17 vector, were grown on LB medium containing 100 μg/ml ampicillin.

Production of Recombinant Proteins

For the production of the recombinant P5βR proteins, bacteria were cultivated at 37°C at 180 rpm on a rotary shaker until an OD_{600} of 0.5–0.7 was reached. Then 0.1 mM isopropyl-β-D-thiogalactoside (IPTG) was added to induce the expression of the recombinant His-tagged fusion protein. The cells were kept at 4°C for up to 96 h under shaking at 100 rpm, after which the His-tagged protein was isolated by nickel-nitrilotriacetic acid (Ni-NTA) agarose purification following the procedure described in the QIAexpressionist handbook (QIAgen,) using an Äkta purifier (GE Healthcare).

The Ni-NTA matrix was washed extensively with 20 mM imidazole (50 mM NaH_2PO_4, 300 mM NaCl, 20 mM imidazole, pH 8.0) before affinity-bound proteins were eluted with 250 mM imidazole (elution buffer: 50 mM NaH_2PO_4, 300 mM NaCl, 250 mM imidazol, pH 8.0). After purification of the recombinant proteins, the elution buffer was exchanged for the incubation buffer using PD-10 columns (GE Healthcare). The incubation buffer consisted of 100 mM HEPES-KOH (pH 8.0), 250 mM sucrose, 2 mM EDTA, and 10 mM β-mercaptoethanol or 20 mM MOPS buffer (pH 7.0). Protein was quantified according to Bradford (1976).

Proteins were separated by SDS-PAGE and semi-dry immunoblotting was performed according to the QIAexpress Detection and Assay Handbooks (QIAgen) with slight modifications. Recombinant proteins were separated on a 12% Bis-Tris polyacrylamide gel and then transferred onto a nitrocellulose membrane by electroblotting. After blocking with 5% milk powder in 1× Tris-buffered saline with 0.1% Tween 20, the membrane was incubated for 1 h with mouse anti-His antibodies (mixture of RGS-, Tetra-, and Penta-His antibodies; dilution 1:2000; QIAgen, Hilden, Germany). Anti-mouse IgG-peroxidase antibody (Sigma, Munich, Germany) was used as the detection antibody (dilution 1:10 000; incubation 1 h). Chemiluminescence of 3-aminophthalate released from luminol was used for detection.

Enzyme Assays for Recombinant P5βRs

To determine the kinetic constants of rP5βR proteins, reductase activity was measured spectrophotometrically. The conversion of NADPH (0.4 mM) (AppliChem GmbH) to $NADP^+$ was monitored at 340 nm in the presence of the respective substrates over a time course of 5 min or 60 s at 40°C. Depending on the rP5βR investigated, between 0.01 and 0.1 mg/ml of recombinant protein, 0.4 mM NADPH, and varying concentrations of the substrate (0.01–0.4 mM) were used in the assay. An assay without the respective substrate was used as control. Progesterone,

Figure 9. Catalytic Pocket of CrP5βR1, CrP5βR2, CrP5βR4, CrP5βR5, and CrP5βR6 Versus DIP5βR Modeled on the Crystal Structure of 2V6G (DIP5βR) with NADPH as Co-factor Created by PyMOL.
The catalytically important amino acids are marked.
(A) Catalytic pocket of DIP5βR with NADPH and docked progesterone; W106/Y179/K147/G145/F153/M215/F353 are catalytically important amino acids in the binding pocket after Bauer et al. (2010).
(B) Catalytic pocket of CrP5βR1 versus DIP5βR.
(C) Catalytic pocket of CrP5βR2 versus DIP5βR.
(D) Catalytic pocket of CrP5βR4 versus DIP5βR.
(E) Catalytic pocket of CrP5βR5 versus DIP5βR.
(F) Catalytic pocket of CrP5βR6 versus DIP5βR.

2-cyclohexen-1-one, and MVK were purchased from Sigma-Aldrich and 8-oxogeranial from Chiralix BV.

For GC–MS analysis of recombinant rP5βR activity, assays were performed in either 100 mM HEPES-KOH (pH 8.0) or 20 mM MOPS (pH 7.0) buffer. The protein concentration was set to 0.05 mg/ml and the substrate concentration was 0.3 mM with a final assay volume of 1 ml. The reaction was stopped with 1 ml dichloromethane after 1 h at 23°C. The reaction products were extracted and the organic phase was evaporated at 23°C. For GC–MS analysis, the samples were dissolved in 100 µl of dichloromethane. The authentic iridodial standard was purchased from Chiralix BV.

GC–MS analysis was carried out in an Agilent 7890A System coupled to an Agilent 5975C MS detector. A J&W GC column (30 m × 0.25 mm × 0.25 µm) and helium gas at 1.2 ml/min was used. The program started at 60°C and ran at 5°C/min up to 150°C, a 20°C/min gradient up to 240°C, 20°C/min up to 290°C, and 5 min isothermal at 290°C.

In Silico Sequence Analysis

For phylogenetic analysis, P5βR protein sequences were aligned with ClustalW and the phylogenetic tree was generated with the MEGA 4.0.1 software (Tamura et al., 2007) by the Neighbor-Joining method, and bootstrapping was done with 1000 replicates. The evolutionary distances were computed with the Poisson correction method, and all positions containing gaps and missing data were eliminated from the data set (complete deletion option).

The SWISS-MODEL software (http://swissmodel.expasy.org) was used for protein structure homology modeling. The three-dimensional structural drawings were created with PyMOL (http://www.pymol.org).

Subcellular Protein Localization

For subcellular protein localization, Gateway recombination of the six CrP5βR entry clones was carried out with the pK7WGF2 vector (Karimi et al., 2002), and the RFP entry clone (Karimi et al., 2007) was Gateway recombined with the pH7WG2 vector (Karimi et al., 2002). The resulting expression clones were transformed into *Agrobacterium tumefaciens* LBA4404 cells. Recombinant *A. tumefaciens* was grown for 2 days in a shaking incubator (150 rpm) at 28°C in 5 ml of yeast extract broth medium, supplemented with appropriate antibiotics (100 µg/ml spectinomycin, 300 µg/ml streptomycin, 100 µg/ml rifampicin, and 20 µg/ml gentamycin). After incubation, the bacterial cultures were diluted five-fold, and incubated for one more day under the same conditions. For co-transformation, 150 µl of each *A. tumefaciens* culture containing a *CrP5βR* expression clone was mixed with 150 µl of *A. tumefaciens* culture containing the *RFP* expression clone. The resulting mixture was transferred to a Petri dish containing 8 ml of a 3-day-old BY-2 culture (BY-2 medium: MS medium [pH 5.8] supplemented with 3% [w/v] sucrose, 0.02% [w/v] monopotassium phosphate, and 0.1% [v/v] BY-2 vitamin solution [0.02 g of 2,4-D; 0.05 g of thiamine, and 5.00 g of myo-inositol in 50 ml of water]). Co-cultivation of BY-2 cells and bacteria was allowed for 2 days at 24°C in the dark, after which the mixture was spread on horizontal Petri dishes containing solid BY-2 medium supplemented with antibiotics (100 µg/ml kanamycin, 30 µg/ml hygromycin, 500 µg/ml carbenicillin, and 200 µg/ml vancomycin). After 3 weeks of incubation at 24°C in the dark, transgenic calli with both red and green fluorescence were selected and subcultured onto new BY-2 plates with antibiotics. For maintenance, transgenic calli were subcultured every 4 weeks onto fresh BY-2 plates and incubated at 24°C in the dark. Confocal laser scanning microscopy was carried out with an LSM 510 confocal microscope (Zeiss) equipped with a 63× water-corrected objective (numerical aperture of 1.2). GFP was excited using 488 nm laser light and imaged using a 505–550 nm BP filter. RFP was excited using 543 nm laser light and imaged using an LP560 filter. For each construct, several independent transgenic calli were analyzed.

In Silico Transcriptome Analysis

Average linkage hierarchical clustering of gene expression profiles from publicly available transcriptomes of *C. roseus* was conducted as described (Van Moerkercke et al., 2013).

In Situ Hybridization

Gene constructs containing the complete cDNA of the *CrP5βR*s, including the 5′ and 3′ untranslated regions (UTRs), were cloned into the pBluescript II SK+ vector using the restriction sites SalI and NotI. The synthesis of antisense and sense digoxigenin-labeled RNA probes was performed as described (Burlat et al., 2004) and the *G8O* and *SGD* antisense probes (Burlat et al., 2004; Guirimand et al., 2010) were used as IPAP and epidermal markers, respectively. Paraffin-embedded serial cross sections of young apex, including developing leaves and flower buds, were hybridized with digoxigenin-labeled RNA probes and localized with anti-digoxigenin antibodies conjugated with alkaline phosphatase (Mahroug et al., 2006). Slides were imaged using a high-resolution slide scanner at ×20 objective lens (0.46 µm/pixel; Nanozoomer 2.0HT, Hamamatsu Photonics, Tokyo, Japan). Image analysis was performed with the Hamamatsu (Tokyo, Japan) Photonics image viewer (NanoZoomer Digital Pathology, NDP) for virtual microscopy. Figures were assembled with images directly extracted from the scans.

Virus-Induced Gene Silencing

All constructs were cloned using Gateway technology (Invitrogen). For the CrP5βR2-pTRV2 construct, the 5′-UTR and 3′-UTR regions were joined by an overlap-PCR strategy. The 5′-UTR and 3′-UTR were PCR amplified using primers 5′-AAAAAGCAGGCTcacccacaggcagctcacgg-3′ (partial AttB1 side capitalized) and 5′-CTAAAGATCAGAggtgagattacaa aattgatg-3′ (3′-UTR overlap region capitalized), and primers 5′- GTAA TCTCACCctgatctttagttagaattgtc-3′ (5′-UTR overlap region capitalized) and 5′- AGAAAGCTGGGTcaaaatatgtgtagttttggttac-3′ (partial AttB2 side capitalized), respectively. Both fragments were fused introducing full-length AttB1/2 sites using primers 5′- ggggacaagtttgtacaaaaaag caggct-3′ and 5′-ggggaccactttgtacaagaaagctgggt-3′. For CrP5βR4 and CrP5βR5, a similar strategy was used with the following primers: 5′-AAAAAGCAGGCTattttctctgaacatttctttg-3′, 5′-CACTAACAAACcttcag gggataatgaaaatgg-3′, 5′-ATCCCCTGAAGgtttgttagtgtctttccttg-3′, and 5′-AGAAAGCTGGGTgattgaagagctcaggaaatg-3′ for CrP5βR4-pTRV2 and primers 5′-AAAAAGCAGGCTagccaagtctttctattgcacattc-3′, 5′-GGA ATAAAACCcttccaccaccaactcattatgtc-3′, 5′-GTGGTGGAAGgtttattcctta gaattttggtg-3′, and 5′-AGAAAGCTGGGTcaccaaacaaaacaaattgcattag-3′ for CrP5βR5-pTRV2. To create the Protoporphyrin IX magnesium chelatase subunit H (ChLH) control construct, primers 5′-GGGGACAAGTTTG TACAAAAAAGCAGGCTgtcagttgccacactagttaatattgctgc-3′ (AttB1 site capitalized) and 5′- GGGGACCACTTTGTACAAGAAAGCTGGGTAgcatg-gatattctttcccgttggc-3′ (AttB2 site capitalized) were used (Liscombe and O'Connor, 2011). All AttB1/2 fragments were recombined into pDONR207 and subsequently into a Gateway-compatible pTRV2 vector (ABRC9080; YL279). Constructs were sequenced and transferred to the *A. tumefaciens* strain GV3101 (pMP90).

VIGS was performed essentially as described by Liscombe and O'Connor (2011) and Geu-Flores et al. (2012) using *C. roseus* cv. Sunstorm Rose. For *CrP5βR4* and *CrP5βR5* co-silencing, agrobacteria were mixed 1:1 before pinching. Plants were grown at 25°C in a 12 h/12 h light/dark cycle and material was harvested when ChlH-pTRV2 plants showed fully bleached leaves. Briefly, leaf tissue was ground using a Retsch ball mill, weighed, collected into 200 µl of methanol containing 40 µM caffeine as an internal standard and incubated at 60°C for 2 h. After a 30 min centrifugation step at 5000 *g*, an aliquot of the supernatant (50 µl) was mixed with an equal volume of water and analyzed on a Thermo-Finnigan instrument equipped with a Deca XP ion trap detector. The column used was a Phenomenex Kinetix 5µ C18 100A (100 × 2.10 mm, 5 µm), and the binary solvent system consisted of acetonitrile (ACN) and 0.1% formic acid in water. The elution program was as follows: 1 min isocratic at 12% ACN, 3.5 min gradient up

to 25% ACN, 2.5 min gradient up to 50% ACN, 1 min gradient up to 100% ACN, 6 min isocratic at 100% ACN, 1 min gradient down to 12% ACN, and 2.5 min isocratic at 12% ACN. Peak areas were calculated using the ICIS algorithm in Finnigan's Xcalibur software and normalized by leaf mass (fresh weight) and the peak area of caffeine.

Total RNA from VIGS leaves was isolated using the RNeasy mini kit (Qiagen) and cDNA synthesized with the iStript cDNA synthesis kit (Bio-Rad). Primers were designed using Primer3 (http://biotools.umassmed.edu/bioapps/primer3_www.cgi) and are shown in Supplemental Table 4. The *C. roseus N2227* (Caros011588.1) and *SAND* (Caros010066.1) genes (Van Moerkercke et al., 2013; http://bioinformatics.psb.ugent.be/orcae/overview/Catro) were used as reference genes and qRT–PCR was performed with a Lightcycler 480 (Roche) using SYBR Green QPCR master Mix (Stratagene). Reactions were performed in triplicate and qBase was used to quantify relative expression (Hellemans et al., 2007).

ACCESSION NUMBERS
Sequence data from this article can be found in the GenBank data libraries under accession numbers KJ873882 (CrP5βR1), KJ873883 (CrP5βR2), KJ873884 (CrP5βR3), KJ873885 (CrP5βR4), KJ873886 (CrP5βR5), KJ873887 (CrP5βR6), KJ873888 (MtP5βR1), KJ873889 (MtP5βR2), KJ873890 (MtP5βR3), and KJ873891 (MtP5βR4).

SUPPLEMENTAL INFORMATION
Supplemental Information is available at *Molecular Plant Online*.

REFERENCES
Alméras, E., Stolz, S., Vollenweider, S., Reymond, P., Mène-Saffrané, L., and Farmer, E.E. (2003). Reactive electrophile species activate defense gene expression in Arabidopsis. Plant J. **34**:205–216.

Asada, K., Salim, V., Masada-Atsumi, S., Edmunds, E., Nagatoshi, M., Terasaka, K., Mizukami, H., and De Luca, V. (2013). A 7-deoxyloganetic acid glucosyltransferase contributes a key step in secologanin biosynthesis in Madagascar periwinkle. Plant Cell **25**:4123–4134.

Bauer, P., Munkert, J., Brydziun, M., Burda, E., Müller-Uri, F., Gröger, H., Muller, Y.A., and Kreis, W. (2010). Highly conserved progesterone 5β-reductase genes (P5βR) from 5β-cardenolide-free and 5β-cardenolide-producing angiosperms. Phytochemistry **71**:1495–1505.

Bauer, P., Rudolph, K., Müller-Uri, F., and Kreis, W. (2012). Vein Patterning 1-encoded progesterone 5β-reductase: activity-guided improvement of catalytic efficiency. Phytochemistry **77**:53–59.

Bradford, M.M. (1976). A rapid and sensitive method for the quantitation of microgram quantities of protein utilizing the principle of protein-dye binding. Anal. Biochem. **72**:248–254.

Burda, E., Kraußer, M., Fischer, G., Hummel, W., Muller-Uri, F., Kreis, W., and Gröger, H. (2009). Recombinant Δ^{4,5}-steroid 5 β-reductases as biocatalysts for the reduction of activated C=C-double bonds in monocyclic and acyclic molecules. Adv. Synth. Catal. **351**:2787–2790.

Burlat, V., Oudin, A., Courtois, M., Rideau, M., and St-Pierre, B. (2004). Co-expression of three MEP pathway genes and geraniol 10-hydroxylase in internal phloem parenchyma of Catharanthus roseus implicates multicellular translocation of intermediates during the biosynthesis of monoterpene indole alkaloids and isoprenoid-derived primary metabolites. Plant J. **38**:131–141.

Courdavault, V., Papon, N., Clastre, M., Giglioli-Guivarc'h, N., St-Pierre, B., and Burlat, V. (2014). A look inside an alkaloid multisite plant: the Catharanthus logistics. Curr. Opin. Plant Biol. **19C**:43–50.

Durchschein, K., Wallner, S., Macheroux, P., Schwab, W., Winkler, T., Kreis, W., and Faber, K. (2012). Nicotinamide-dependent ene reductases as alternative biocatalysts for the reduction of activated alkenes. Eur. J. Org. Chem. **26**:4963–4968.

Gärtner, D.E., Keilholz, W., and Seitz, H.U. (1994). Purification, characterization and partial peptide microsequencing of progesterone 5β-reductase from shoot cultures of Digitalis purpurea. Eur. J. Biochem. **225**:1125–1132.

Gavidia, I., Tarrío, R., Rodríguez-Trelles, F., Pérez-Bermúdez, P., and Seitz, H.U. (2007). Plant progesterone 5β-reductase is not homologous to the animal enzyme. Molecular evolutionary characterization of P5βR from Digitalis purpurea. Phytochemistry **68**:853–864.

Geu-Flores, F., Sherden, N.H., Courdavault, V., Burlat, V., Glenn, W.S., Wu, C., Nims, E., Cui, Y., and O'Connor, S.E. (2012). An alternative route to cyclic terpenes by reductive cyclization in iridoid biosynthesis. Nature **492**:138–142.

Guirimand, G., Courdavault, V., Lanoue, A., Mahroug, S., Guihur, A., Blanc, N., Giglioli-Guivarc'h, N., St-Pierre, B., and Burlat, V. (2010). Strictosidine activation in Apocynaceae: towards a "nuclear time bomb"? BMC Plant Biol. **10**:182.

Hellemans, J., Mortier, G., De Paepe, A., Speleman, F., and Vandesompele, J. (2007). qBase relative quantification framework and software for management and automated analysis of real-time quantitative PCR data. Genome Biol. **8**:R19.

Herl, V., Fischer, G., Müller-Uri, F., and Kreis, W. (2006). Molecular cloning and heterologous expression of progesterone 5β-reductase from Digitalis lanata Ehrh. Phytochemistry **67**:225–231.

Herl, V., Fischer, G., Reva, V.A., Stiebritz, M., Muller, Y.A., Müller-Uri, F., and Kreis, W. (2009). The VEP1 gene (At4g24220) encodes a short-chain dehydrogenase/reductase with 3-oxo-Δ^{4,5}-steroid 5β-reductase activity in Arabidopsis thaliana L. Biochimie **91**:517–525.

Jörnvall, H., Persson, B., Krook, M., Atrian, S., Gonzàlez-Duarte, R., Jeffery, J., and Ghosh, D. (1995). Short-chain dehydrogenases reductases (SDR). Biochemistry **34**:6003–6013.

Karimi, M., Bleys, A., Vanderhaeghen, R., and Hilson, P. (2007). Building blocks for plant gene assembly. Plant Physiol. **145**:1183–1191.

Karimi, M., Inzé, D., and Depicker, A. (2002). GATEWAY^{TM} vectors for Agrobacterium-mediated plant transformation. Trends Plant Sci. **7**:193–195.

Kavanagh, K., Jörnvall, H., Persson, B., and Oppermann, U. (2008). The SDR superfamily: functional and structural diversity within a

family of metabolic and regulatory enzymes. Cell. Mol. Life Sci. **65**:3895–3906.

Kreis, W., Hensel, A., and Stuhlemmer, U. (1998). Cardenolide biosynthesis in foxglove. Planta Med. **64**:491–499.

Liscombe, D.K., and O'Connor, S.E. (2011). A virus-induced gene silencing approach to understanding alkaloid metabolism in Catharanthus roseus. Phytochemistry **72**:1969–1977.

Mahroug, S., Courdavault, V., Thiersault, M., St-Pierre, B., and Burlat, V. (2006). Epidermis is a pivotal site of at least four secondary metabolic pathways in Catharanthus roseus aerial organs. Planta **223**:1191–1200.

Miettinen, K., Dong, L., Navrot, N., Schneider, T., Burlat, V., Pollier, J., Woittiez, L., van der Krol, S., Lugan, R., Ilc, T., et al. (2014). The seco-iridoid pathway from Catharanthus roseus. Nat. Commun. **5**:3606.

Munkert, J., Bauer, P., Burda, E., Müller-Uri, F., and Kreis, W. (2011). Progesterone 5β-reductase of Erysimum crepidifolium: cDNA cloning, expression in Escherichia coli, and reduction of enones with the recombinant protein. Phytochemistry **72**:1710–1717.

Ober, D. (2010). Gene duplications and the time thereafter – examples from plant secondary metabolism. Plant Biol. **12**:570–577.

Pérez-Bermúdez, P., García, A.A.M., Tuñón, I., and Gavidia, I. (2010). Digitalis purpurea P5βR2, encoding steroid 5β-reductase, is a novel defense-related gene involved in cardenolide biosynthesis. New Phytol. **185**:687–700.

Renault, H., Bassard, J.-E., Hamberger, B., and Werck-Reichhart, D. (2014). Cytochrome P450-mediated metabolic engineering: current progress and future challenges. Curr. Opin. Plant Biol. **19**:27–34.

Salim, V., Wiens, B., Masada-Atsumi, S., Yu, F., and De Luca, V. (2014). 7-Deoxyloganetic acid synthase catalyzes a key 3 step oxidation to form 7-deoxyloganetic acid in Catharanthus roseus iridoid biosynthesis. Phytochemistry **101**:23–31.

Salim, V., Yu, F., Altarejos, J., and De Luca, V. (2013). Virus-induced gene silencing identifies Catharanthus roseus 7-deoxyloganic acid-7-hydroxylase, a step in iridoid and monoterpene indole alkaloid biosynthesis. Plant J. **76**:754–765.

Schuler, M.A., and Werck-Reichhart, D. (2003). Functional genomics of P450s. Annu. Rev. Plant Biol. **54**:629–667.

St-Pierre, B., Vazquez-Flota, F.A., and De Luca, V. (1999). Multicellular compartmentation of Catharanthus roseus alkaloid biosynthesis predicts intercellular translocation of a pathway intermediate. Plant Cell **11**:887–900.

Tamura, K., Dudley, J., Nei, M., and Kumar, S. (2007). MEGA4: molecular evolutionary genetics analysis (MEGA) software version 4.0. Mol. Biol. Evol. **24**:1596–1599.

Tarrío, R., Ayala, F.J., and Rodríguez-Trelles, F. (2011). The Vein Patterning 1 (VEP1) gene family laterally spread through an ecological network. PLoS ONE **6**:e22279.

Thorn, A., Egerer-Sieber, C., Jäger, C.M., Herl, V., Müller-Uri, F., Kreis, W., and Muller, Y.A. (2008). The crystal structure of progesterone 5β-reductase from Digitalis lanata defines a novel class of short chain dehydrogenases/reductases. J. Biol. Chem. **283**:17260–17269.

van der Fits, L., and Memelink, J. (2000). ORCA3, a jasmonate-responsive transcriptional regulator of plant primary and secondary metabolism. Science **289**:295–297.

Van Moerkercke, A., Fabris, M., Pollier, J., Baart, G.J.E., Rombauts, S., Hasnain, G., Rischer, H., Memelink, J., Oksman-Caldentey, K.M., and Goossens, A. (2013). CathaCyc, a metabolic pathway database built from Catharanthus roseus RNA-Seq data. Plant Cell Physiol. **54**:673–685.

Zhang, Y., Teoh, K.H., Reed, D.W., Maes, L., Goossens, A., Olson, D.J.H., Ross, A.R.S., and Covello, P.S. (2008). The molecular cloning of artemisinic aldehyde Δ11(13) reductase and its role in glandular trichome-dependent biosynthesis of artemisinin in Artemisia annua. J. Biol. Chem. **283**:21501–21508.